

# Identification of Harmonic Source Location in Power Distribution Network

*by Mohd Hatta Jopri*

---

**Submission date:** 06-Feb-2022 12:30PM (UTC+0800)

**Submission ID:** 1755746083

**File name:** Identification-Turnitin.docx (1.95M)

**Word count:** 2829

**Character count:** 14860



## Identification of Harmonic Source Location in Power Distribution Network

Mohd Hatta Jopri<sup>1</sup>, Aleksandr Skamyin<sup>2</sup>, Mustafa Manap<sup>3\*</sup>, Tole Sutikno<sup>4</sup>,  
Mohd Riduan Mohd Shariff<sup>5</sup>, Aleksey Belsky<sup>6</sup>

<sup>1,2</sup>Faculty of Electrical & Electronic Engineering Technology, Universiti Teknikal Malaysia Melaka, Malaysia  
<sup>3</sup>Department of Electric Power and Electromechanics, Saint Petersburg Mining University, Saint Petersburg, Russia  
<sup>4</sup>Department of Electrical Engineering, Universitas Ahmad Dahlan, Yogyakarta, Indonesia  
<sup>5</sup>Electrical Section, Engineering Department, Malaysian Refining Company Sdn. Bhd.  
<sup>6</sup>Electromechanical Department, Saint Petersburg Mining University, Saint Petersburg, Russia

### Article Info

#### Article history:

Received mm dd, yyyy  
Revised mm dd, yyyy  
Accepted mm dd, yyyy

#### Keywords:

Harmonic source location  
Time-frequency distribution  
S-transform  
TFR impedance  
Spectral impedance

### ABSTRACT

This paper presents the experimental setup of identification of harmonic source location in the power distribution network using time-frequency analysis, known as S-transform (ST) at the point of common coupling (PCC). S-transform offers high frequency resolution in analyzing the low frequency component and able to represent signal parameters in time-frequency representation (TFR) such as TFR impedance ( $Z_{TFR}$ ). The proposed method is based on IEEE Std. 1459-2010, ST, and the significant relationship of spectral impedances components ( $Z_s$ ) that been extracted from the  $Z_{TFR}$ , consist of the fundamental impedance ( $Z_f$ ) and harmonic impedance ( $Z_h$ ). This experiment was conducted out on an IEEE 4-bus test feeder with a harmonic producing load in numerous different scenarios. The experimental was tested and verified for three consecutive months. The findings of this study reveal that the proposed method provides 100 percent correct identification of harmonic source location.

**2**

This is an open access article under the [CC BY-SA](#) license.



### Corresponding Author:

Mustafa Manap,  
Faculty of Electrical & Electronic Engineering Technology,  
Universiti Teknikal Malaysia Melaka (UTeM),  
Melaka, Malaysia.  
Email: [mustafa@utem.edu.my](mailto:mustafa@utem.edu.my)

### 1. INTRODUCTION

Due to the rise of harmonic-producing loads, harmonic distortion has become one of the primary power quality concerns [1], [2]. Harmonic distortion, which causes voltage and current waveforms to be distorted and contain various harmonic orders, is one of the most common types of disturbances [3]–[6]. The power system is impacted by the disturbances; therefore, monitoring is required to limit the impacts, which may include equipment failures due to overheating, reduced transformer life expectancy due to deterioration of insulation levels, and increased equipment power losses [7]–[10]. Moreover, harmonics can cause overheating and damage to end-user equipment, as well as have unfavorable effects on the power system. As a result, it is critical for a power system operator to understand the system's harmonic behavior [11]–[13]. As mentioned in [14]–[18], harmonic sources, on the other hand, have complicated properties such as nonlinearity and abrupt variations that are difficult to forecast using standard methods. The foremost common circumstance that needs harmonic source location is to settle the disputes over who is responsible for harmonic distortions, whether it comes upstream or downstream of the PCC [19]–[21].

The power direction method is the most popular method of identifying harmonic sources [22]–[24]. Next, the critical impedance method based on reactive power [25], [26] also offers a certain level of accuracy. Some basic assumptions are required for the approaches listed above, such as prior knowledge of source impedance [11], [27]–[29]. In contrast of active power flow direction, the reactive power methods provide always correct claims with regards to the dominant equivalent harmonic source. These approaches, however, is unable to establish the harmonic contribution of each side [30]–[34]. Other methods, such as fluctuation and regression methods, require that the major harmonic source be on the customer side and that the background harmonic voltage required to be stable [35]–[39]. Furthermore, approaches based on the detection of total harmonic distortion are insensitive to changes in the phase angle of the harmonic source, making it impossible to precisely establish the source of harmonic distortion [40]–[42]. According to reference [43], current techniques have been used to identify the harmonic contributions of the customer and the utility in order to detect the harmonic source. Based on the reference impedance as in [34], [44]–[47], a harmonic vector approach has been suggested to determine the utility and customer's harmonic contributions at the PCC. This method allowed for the calculation of harmonic contributions without determining customer impedance, and also improved the findings in resonance situations. The independent component analysis (ICA) methods were utilized in recent research [47]–[50], which need the impedance on the customer's side to be higher than the one on the utility side. However, when the network contains filters or capacitors on the customer side, this is impractical [7], [51].

Short-Time Fourier Transform (STFT) and Stockwell Transform, or S-transform (ST), are the most common time–frequency domain transforms employed in harmonic signal detection approaches [52]–[58]. As explained in [59]–[62], STFT on the one hand, has some disadvantages such as, this transform is window-dependent and has a fixed resolution based on the window size. Furthermore, because the STFT is an Fourier transform (FT) based technique, it may have issues with the picket-fence effect [63], [64]. ST, on the other hand, because it is a multiresolution spectrum analysis technique, does not have these issues [65]–[68]. As a result, ST appears to be a potential transform for power system protection [27]. Because it incorporates information in both the temporal and frequency domains, the ST has shown to be effective in harmonic signal identification approaches [69]. Thus, this paper proposes an experimental setup based on IEEE Std.1459-2010 and ST due to identify the harmonic source location.

## 2. METHODOLOGY

### 2.1 Proposed method

The identification of harmonic source location is divided into five steps, as indicated in Figure 1. The signals are first measured for both voltage and current at the PCC of the network system. Second, four specific instances were explored for recognising harmonic sources on IEEE 4-bus test feeders. The TFR analysis was done on the PCC's voltage and current measurements in the third step ( $V_{PCC}$  and  $I_{PCC}$ ). This analysis yielded the impedance TFR ( $Z_{TFR}$ ), which was then used to calculate the impedance spectral ( $Z_S$ ) components by calculating the values of the  $Z_{TFR}$  components. Finally, the significant association between the fundamental impedance ( $Z_I$ ) and harmonic impedance ( $Z_h$ ) components of impedance spectrum ( $Z_S$ ) components was observed and employed for harmonic source detection. In this experiment, a harmonic generating load was chosen with an amplitude modulation index ( $m_a$ ) of 1.0, a frequency modulation index ( $m_f$ ) of 90, and an input frequency ( $f_i$ ) of 50hz [70]–[73].

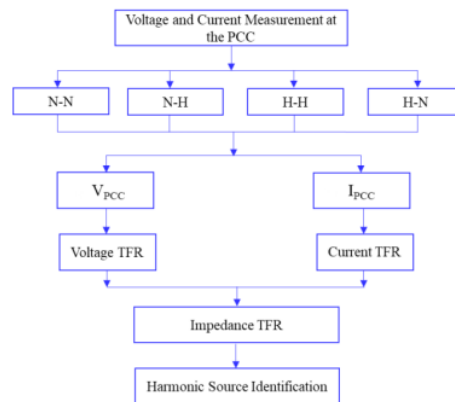


Figure 1. The implementation of the harmonic source identification method

The IEEE 4-bus test feeder is chosen and illustrated in Figures 2 and 3 in order to detect the harmonic source location in the power distribution network in consideration of upstream and downstream of the PCC.

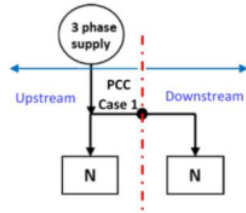


Figure 2. An upstream-downstream for Case 1

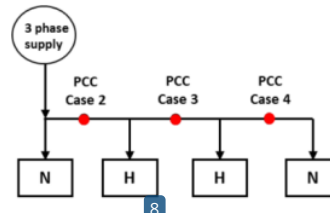


Figure 3. Case 2, 3 and 4

where N is a non-harmonic source which is the resistor load, and H is the harmonic producing load.

In order to test and evaluate the proposed method, an experimental setup was built up in an advanced digital signal processing (ADSP) research facility, as illustrated in Figure 4.

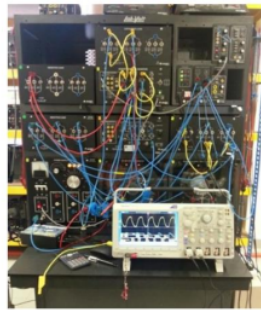


Figure 4. Experimental setup of the proposed system

## 2.2 S-transform

The S-transform (ST) is hybrid of wavelet transform (WT) and the short-time Fourier transform (STFT), which inherits the advantages of both in signal processing [74], [75]. In the transformation process, ST uses a moving and scalable localising Gaussian window in particular. ST can be defined as follows:

$$ST(\tau, f) = \int_{-\infty}^{\infty} x(t) \frac{|f|}{\sqrt{2\pi}} e^{-\frac{(\tau-t)^2 f^2}{2}} e^{-j2\pi ft} dt \quad (1)$$

$$\sigma(f) = \frac{1}{|f|}; \quad g(t) = \frac{1}{\sigma\sqrt{2\pi}} e^{-\frac{t^2}{2\sigma^2}} \quad (2)$$

where  $x(t)$  is the signal,  $t$  is the time,  $f$  is the frequency,  $g(t)$  is the scalable Gaussian window, and  $\sigma(t)$  is a parameter that controls the position of the Gaussian window.

### 2.2.1 Signal parameters

The TFR is used to determine the signal parameters of power quality. Furthermore, the instantaneous value is used in the analysis to obtain real-time parameters [76].

#### a) Instantaneous RMS voltage

The root-mean square (RMS) voltage of signal ( $V_{rms}(t)$ ) can be obtained from the sampled waveform, and written as [77], [78],

$$V_{rms}(t) = \sqrt{\int_0^{f_s} P_x(t, f) df} \quad (3)$$

### 1 b) Instantaneous RMS fundamental voltage

The instantaneous RMS fundamental voltage ( $V_{1rms}(t)$ ) can be computed as [79],

$$V_{1rms}(t) = \sqrt{2 \int_{f_{lo}}^{f_{hi}} P_x(t, f) df} \quad (4)$$

$$f_{hi} = f_0 + 25 \text{ Hz}; f_{lo} = f_0 - 25 \text{ Hz}$$

where  $P_x$  is the power spectrum obtained from the TFR of signal and  $f_0$  is the fundamental frequency corresponding to the power system frequency.

### 2.2.2 Impedance TFR analysis

The impedance TFR ( $Z_{TFR}$ ) offered useful information about the frequency response of the system, as well as harmonic points and possible issues caused by harmonic distortions. The desired current harmonic data and the difference in voltage harmonic data at the location of interest have to be measured in order to determine the impedance TFR. The  $Z_{TFR}$  at each harmonic frequency was calculated using this data, and the results were shown [80]. The  $Z_{TFR}$  equation can be expressed as,

$$Z_{TFR} = \frac{S_V(t, f)}{S_I(t, f)} \quad (5)$$

where  $S_V(t, f)$  signifies the TFR of voltage and  $S_I(t, f)$  signifies the TFR of current.

### 4 2.2.3 Spectral impedance

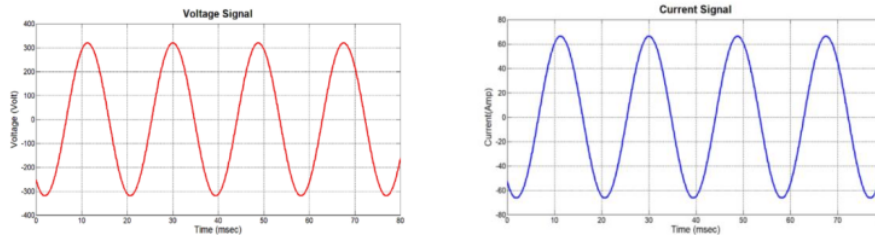
The spectral impedance ( $Z_S$ ) comprises the fundamental impedance ( $Z_I$ ) and harmonic impedance ( $Z_h$ ) that is obtained from  $Z_{TFR}$  [81]. The fundamental impedance ( $Z_I$ ) was an impedance at 50 Hz, which was the frequency of the power source. In the meantime, harmonic impedance ( $Z_h$ ) was a harmonic impedance with an order of harmonics.

## 3 RESULTS AND DISCUSSION

The implementation of the proposed technique initially done by measuring the voltage and current signals at PCC with consideration of 4 specific cases as discussed in 2.1. The location of harmonic sources can be distinguished by analyzing the significant relationship between  $Z_I$  and  $Z_h$ , accordingly.

### 3.1 Case 1: No harmonic source

Only the linear loads were placed upstream and downstream of the PCC in case 1. The voltage signal in the time domain, as well as its voltage TFR, are shown in Figures 5 (a) and (b). The maximum voltage was 342.5 V, while the maximum current was 66.5 A. Meanwhile, Figures 5 (c) and (d) illustrate the TFR of voltage and current signals derived from S-transform analysis. The higher the magnitude, the redder the colour bar, and the lower the magnitude, the bluer the colour bar. There were no other components in the signals and the largest magnitude was only seen at 50 Hz. The results showed that there were no harmonic components in the signal.



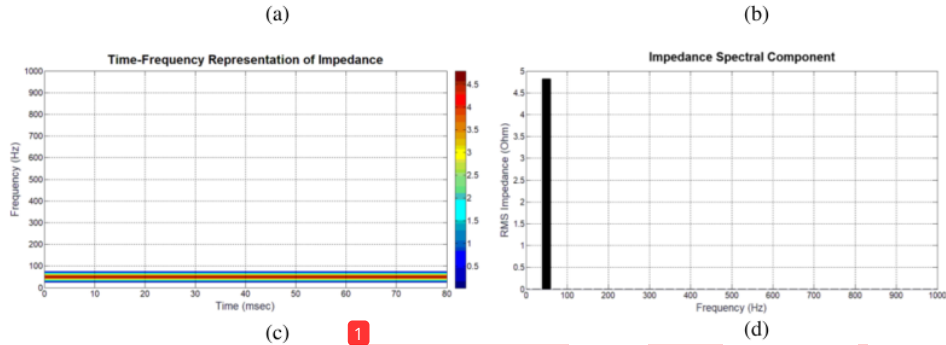


Figure 5. Case 1, (a) voltage signal in time domain, (b) current signal in time-domain, (c) TFR impedance using S-transform, (d) spectral impedance

The  $Z_I$  existed at 50 Hz with a resistance of 4.8 ohm and no harmonic components in the signal, as shown in Figure 5 (d). Thus, in case 1, the significant relationship between  $Z_I$  and  $Z_h$  in the power system network at no harmonic producing load can be expressed as,

$$Z_I \neq 0 \text{ ohm} \tag{5}$$

$$Z_h = 0 \text{ ohm} \tag{6}$$

where for harmonic component,  $h$  is any positive integer, whereas for interharmonic,  $h$  is any positive non-integer.

### 3.2 Case 2: Harmonic source located at PCC's downstream

The linear load is positioned upstream of the PCC in case 2, while the harmonic load is located downstream. The TFR of voltage and current signals derived from the S-transform analysis is shown in Figure 6 (a) and (b). It can be seen that the harmonic and interharmonic components exist between 200 and 1000 Hz, whereas the fundamental components of voltage and current have the maximum magnitudes at 50 Hz. The  $Z_{TFR}$  is calculated using equation 5 in Figure 6 (c), and the figure demonstrates that impedance components occur at frequencies of 50 Hz, 275 Hz, 375 Hz, 600 Hz, 700 Hz, and 900 Hz, respectively. The  $Z_S$  is then derived by calculating the parameters of the ZTFR, as shown in Figure 6. (d).

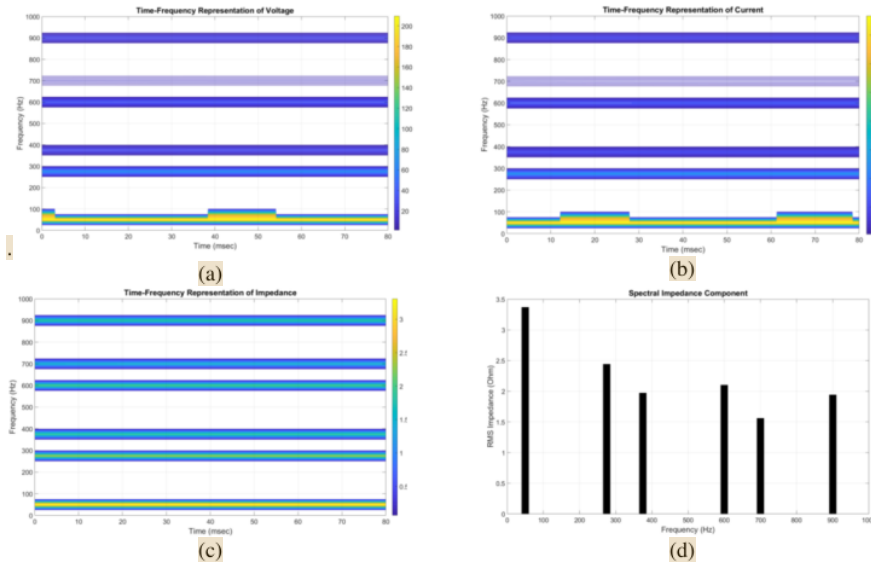


Figure 6. Case 2, (a) voltage signal in TFR using S-transform, (b) current signal in TFR using S-transform, (c) TFR impedance using S-transform, (d) spectral impedance



Table 1 summarises the  $Z_S$  characteristics shown in Figure 6 (d). The  $Z_I$  value is always higher than any  $Z_h$  components, as can be seen.

Table 1. The spectral impedance components for Case 2

Spectral impedance	Ohm
$Z_I$	3.4
$Z_{275}$	2.5
$Z_{375}$	2.0
$Z_{600}$	2.1
$Z_{700}$	1.5
$Z_{900}$	2.0

The relationship between the  $Z_S$  components can be used to identify the location of harmonic sources, according to the findings. As a result, in instance 2, the significant relationship between  $Z_I$  and  $Z_h$  at the condition of the harmonic source downstream of the PCC can be stated as,

$$Z_I \neq 0 \text{ ohm} \quad (7)$$

$$Z_h < Z_I \quad (8)$$

where for harmonic component,  $h$  is any positive integer whereas, for interharmonic,  $h$  is any positive non-integer.

### 3.3 Case 3: Harmonic sources located at PCC's upstream and downstream

The TFR of voltage and current signals derived from the S-transform analysis for case 3 is shown in Figures 7 (a) and 7 (b). It can be seen that 7<sup>th</sup> harmonic and interharmonic components occur in the frequency range of 200 Hz to 1000 Hz, whereas the fundamental components of voltage and current, respectively, have the maximum magnitudes at 50 Hz. The voltage and current waveforms can be seen to be distorted due to the harmonic load located upstream and downstream of the PCC. The  $Z_{TFR}$  is calculated using equation 5 in Figure 7 (c), and the figure demonstrates that impedance components occur at frequencies of 50 Hz, 275 Hz, 375 Hz, 600 Hz, 700 Hz, and 900 Hz, respectively. The ZS is then calculated by estimating the parameters of the  $Z_{TFR}$ , as shown in Figure 7. (d).

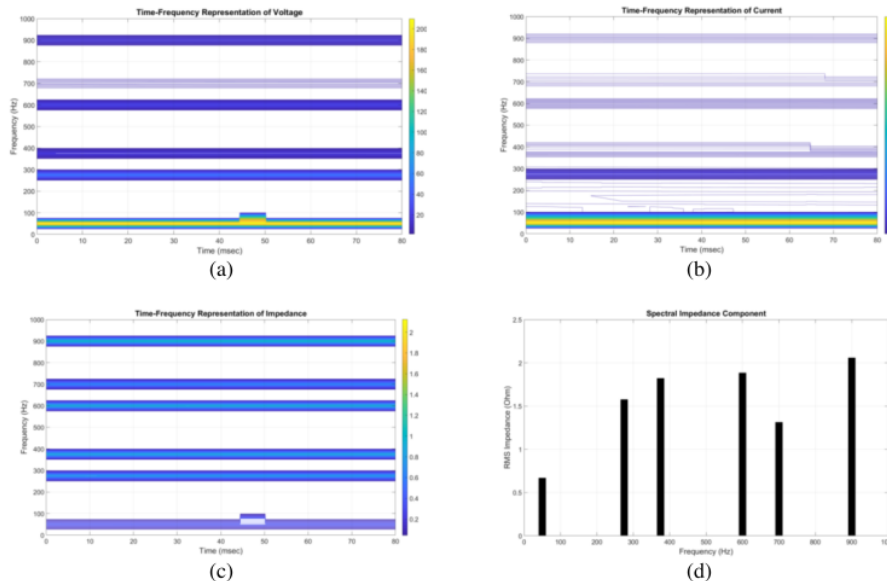


Figure 7. Case 3, (a) voltage signal in TFR using S-transform, (b) current signal in TFR using S-transform, (c) TFR impedance using S-transform, (d) spectral impedance

Table 2 summarises the  $Z_S$  characteristics shown in Figure 7 (d). The  $Z_I$  value is always lower than any  $Z_h$  components, as can be shown.

Table 2. The spectral impedance components for Case 3

Spectral impedance	Ohm
$Z_I$	0.7
$Z_{275}$	1.6
$Z_{375}$	1.8
$Z_{600}$	1.9
$Z_{700}$	1.4
$Z_{900}$	2.1

The relationship between the  $Z_S$  components can be utilised to pinpoint the location of harmonic sources, according to the findings. As a result, in case 3, the significant relationship between  $Z_I$  and  $Z_h$  at the condition of the harmonic source positioned upstream and downstream of the PCC may be expressed as follows:

$$Z_I \neq 0 \text{ ohm} \quad (9)$$

$$Z_h > Z_I \quad (10)$$

where for harmonic component,  $h$  is any positive integer whereas, for interharmonic,  $h$  is any positive non-integer.

### 3.4 Case 4: Harmonic source located at PCC's upstream

The harmonic load is positioned upstream of the PCC in case 4. Figures 8 (a) and (b) illustrate the voltage and current signals acquired from S-transform analysis in the TFR. Between 200 Hz and 1000 Hz, the lowest-magnitude harmonic and interharmonic components are present, with the maximum component magnitude at 50 Hz. The  $Z_{TFR}$  is calculated using equation 5 in Figure 8 (c), and the figure demonstrates that impedance components occur at frequencies of 50 Hz, 275 Hz, 375 Hz, 600 Hz, 700 Hz, and 900 Hz, respectively. The  $Z_S$  is then calculated by estimating the parameters from the  $Z_{TFR}$ , as shown in Figure 8. (d).

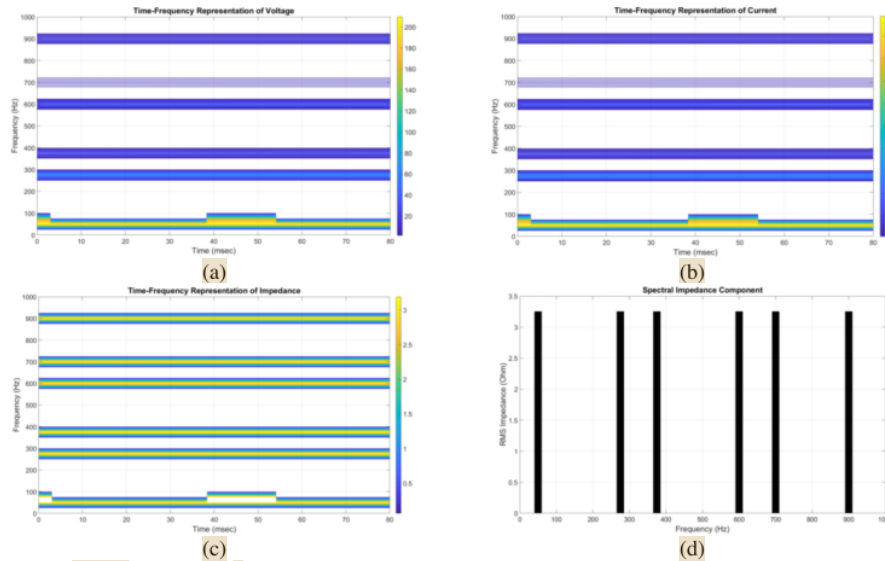


Figure 8. Case 4, (a) voltage signal in TFR using S-transform, (b) current signal in TFR using S-transform, (c) TFR impedance using S-transform, (d) spectral impedance ( $Z_S$ )

Table 3 summarizes the  $Z_S$  characteristics shown in Figure 8 (d). The  $Z_I$  value is the same for all  $Z_h$  components, as can be observed.



Table 3. The spectral impedance components for case 4

Spectral impedance	Ohm
$Z_1$	3.3
$Z_{375}$	3.3
$Z_{375}$	3.3
$Z_{600}$	3.3
$Z_{700}$	3.3
$Z_{900}$	3.3

At the condition of the harmonic source positioned upstream of the PCC, the significant relationship between  $Z_1$  and  $Z_1$  can be stated as,

$$Z_1 \neq 0 \text{ ohm} \quad (11)$$

$$Z_h = Z_1 \quad (12)$$

where for harmonic component,  $h$  is any positive integer whereas, for interharmonic,  $h$  is any positive non-integer.

Furthermore, the proposed method was tried and verified on an experimental setup in October, November, and December 2021, with the harmonic producing load in the linear area (amplitude modulation index is  $0 \leq ma \leq 1$  and inverter switching frequency range is between 2 kHz and 15 kHz) [82]–[86]. Surprisingly, as demonstrated in Figure 9, the proposed method offers 100 percent accurate harmonic source location detection.

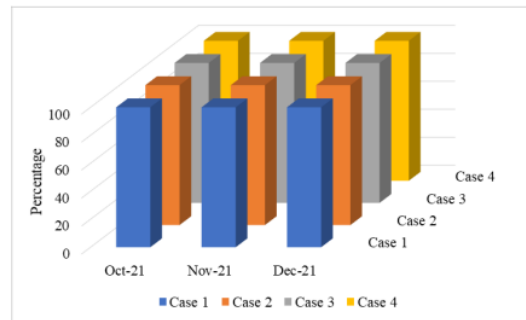


Figure 9. The correctness of the proposed method

### 3. CONCLUSION

The major contribution of this study is the discovery of a significant relationship between  $Z_S$  components that acquired from S-transform analysis in locating harmonic source location. According to Table 4, the proposed method is 100 percent correct in each scenario, and the significant relationship of  $Z_S$  for harmonic source location identification is summarised as follows:

Table 4. Result of proposed method

$Z_1$	$Z_h$	Remark
$Z_1 \neq 0 \text{ ohm}$	$Z_h = 0$	Case 1: No harmonic source
$Z_1 \neq 0 \text{ ohm}$	$Z_h < Z_1$	Case 2: Harmonic source located at PCC downstream
$Z_1 \neq 0 \text{ ohm}$	$Z_h > Z_1$	Case 3: Harmonic source located at upstream and downstream of PCC
$Z_1 \neq 0 \text{ ohm}$	$Z_h = Z_1$	Case 4: Harmonic source located at PCC downstream

### ACKNOWLEDGEMENTS

# Identification of Harmonic Source Location in Power Distribution Network

## ORIGINALITY REPORT

15%

SIMILARITY INDEX

8%

INTERNET SOURCES

14%

PUBLICATIONS

9%

STUDENT PAPERS

## PRIMARY SOURCES

1	Submitted to Universiti Teknikal Malaysia Melaka Student Paper	4%
2	beei.org Internet Source	3%
3	Submitted to Udayana University Student Paper	2%
4	M. H. Jopri, A. R. Abdullah, M. Manap, T. Sutikno, M. R. Ab Ghani. "An Identification of Multiple Harmonic Sources in a Distribution System by Using Spectrogram", Bulletin of Electrical Engineering and Informatics, 2018 Publication	1%
5	Fred, Ana, and Maria De Marsico. "Advances in pattern recognition applications and methods", Neurocomputing, 2016. Publication	1%
6	www.math.ubc.ca Internet Source	1%

7

A.A. Girgis, D.G. Hart, W.L. Peterson. "A new fault location technique for two- and three-terminal lines", IEEE Transactions on Power Delivery, 1992

Publication

1 %

8

M. H Jopri, MR Ab Ghani, A.R Abdullah, Tole Sutikno, M Manap, J. Too. "Naïve Bayes and linear discriminate analysis based diagnostic analytic of harmonic source identification", Indonesian Journal of Electrical Engineering and Computer Science, 2020

Publication

1 %

9

[ijpeds.iaescore.com](http://ijpeds.iaescore.com)

Internet Source

1 %

10

M.H. Jopri, A.R. Abdullah, M. Manap, M.R. Yusoff, T. Sutikno, M.F. Habban. "An Improved of Multiple Harmonic Sources Identification in Distribution System with Inverter Loads by Using Spectrogram", International Journal of Power Electronics and Drive Systems (IJPEDS), 2016

Publication

1 %

11

N. Mat Kassim, A. R. Abdullah, A. F. A Kadir, M. H. Jopri, N. H. Shamsudin. "Performance verification of real-time harmonic sources identification system", 2016 IEEE International Conference on Power and Energy (PECon), 2016

1 %

## Publication

---

Exclude quotes Off

Exclude bibliography Off

Exclude matches < 1%